AIAA 93–0114

An Application of Dynamical Systems Theory to Nonlinear Combustion Instabilities

Craig C. Jahnke
Clarkson University
Potsdam, New York

and

F. E. C. Culick
California Institute of Technology
Pasadena, California

31st Aerospace Sciences Meeting & Exhibit
January 11-14, 1993 / Reno, NV

AN APPLICATION OF DYNAMICAL SYSTEMS THEORY TO NONLINEAR COMBUSTION INSTABILITIES

Craig C. Jahnke
Assistant Professor of Mechanical and Aeronautical Engineerng, Member AIAA
Clarkson University

and

F. E. C. Culick
Professor of Jet Propulsion and Mechanical Engineering, Fellow AIAA
California Institute of Technology

Abstract

Two important approximations have been incorporated in much of the work with approximate analysis of unsteady motions in combustion chambers: truncation of the series expansion to a finite number of modes, and time averaging. A major purpose of the analysis reported in this paper has been to investigate the limitations of those approximations. In particular two fundamental problems of nonlinear behavior are discussed: the conditions under which stable limit cycles of a linearly unstable system may exist; and conditions under which bifurcations of the limit cycle may occur. A continuation method is used to determine the limit cycle behavior of the equations representing the time dependent amplitudes of the longitudinal acoustic modes in a cylindrical combustion chamber. The system includes all linear processes and second-order nonlinear gas dynamics. The results presented show that time averaging works well only when the system is, in some sense, only slightly unstable. In addition, the stability boundaries predicted by the two-mode approximation are shown to be artifacts of the truncation of the system. Systems of two, four, and six modes are analyzed and show that more modes are needed to analyze more unstable systems. For the six-mode approximation with an unstable second mode two bifurcations are found to exist. A pitchfork bifurcation causes a new branch of limit cycles to exist in which the odd acoustic modes are excited. This new branch of limit cycles then undergoes a torus bifurcation that causes the system to exhibit stable quasi-periodic motions.

I. Introduction

Because combustion instabilities arise normally as linearly unstable motions, nonlinear processes must be present to prevent the instabilities from growing without limit. Experimentally, therefore, nonlinear behavior is always observed and serious analysis of nonlinear combustion instabilities began with work by Crocco, Sirignano, Mitchell and Zinn at Princeton in the 1960s. The results reported here are the most recent in continuing investigation begun in the early 1970s, using a form of Galerkin's method.

This approach is based on expressing any unsteady motion in a combustion chamber as a synthesis of normal modes for the geometry in question. Spatial averaging converts the problem of solving the system of nonlinear partial differential equations to the much simpler problem of solving a system of nonlinearly coupled ordinary differential equations for the time-dependent amplitudes of the normal modes. Various tests have confirmed that accurate results can be obtained with this procedure for a broad range of conditions. Hence this system of equations, representing a collection of nonlinear oscillators, seems to be an acceptable formulation for studying various aspects of observed behavior understood poorly or not at all.

There are two main classes of nonlinear problems in this subject: determining the conditions for existence and stability of limit cycles; and determining the conditions under which a linearly stable system may become unstable when subjected to an appropriate disturbance. As a practical matter, two approximations have commonly been used to simplify the analysis and to try to obtain simpler methods for routine applications: (1) time averaging converts the second-order equations to a first-order system governing the slowly changing amplitudes and phases of the modes; and (2) in any case the expansion must be truncated to a finite number of modes. It seems that the possible consequences and validity of those approximations can be understood only by solving the original system of second-order equations. One approach is simply to compute numerical simulations for ranges of the parameters characterizing the system. That tends to be a somewhat arbitrary approach. We choose here to apply some elementary notions of dynamical systems theory and construct bifurcation diagrams. Numerical simulations are then computed only for particularly interesting cases. We believe that this will provide a more systematic approach to understanding the matter cited above.

The equations analyzed in this paper represent the time evolution of the amplitudes of the longi-

tudinal acoustic modes in a cylindrical combustion chamber. Linear contributions from the combustion processes, gas/particle interactions, boundary conditions, and the interaction between the steady and unsteady flow fields are included along with nonlinear contributions from the gas dynamics. The equations were obtained from Paparizos and Culick[1] and have the form

$$\ddot{\eta}_n + \omega_n^2\,\eta_n = 2\,\alpha_n\,\dot{\eta}_n + 2\,\theta_n\,\omega_n\,\eta_n - \sum_{i=1}^{n-1}\left(C_{ni}^{(1)}\,\dot{\eta}_i\,\dot{\eta}_{n-i} + D_{ni}^{(1)}\,\eta_i\,\eta_{n-i}\right) - 2\sum_{i=1}^{\infty}\left(C_{ni}^{(2)}\,\dot{\eta}_i\,\dot{\eta}_{n+i} + D_{ni}^{(2)}\,\eta_i\,\eta_{n+i}\right) \tag{1.1}$$

where

$$C_{ni}^{(1)} = \frac{-1}{2\,\gamma\,i\,(n-i)}\left[n^2 + i\,(n-i)(\gamma-1)\right]$$
$$C_{ni}^{(2)} = \frac{1}{2\,\gamma\,i\,(n+i)}\left[n^2 - i\,(n+i)(\gamma-1)\right]$$
$$D_{ni}^{(1)} = \frac{(\gamma-1)\,\omega_1^2}{4\,\gamma}\left[n^2 - 2\,i\,(n-i)\right]$$
$$D_{ni}^{(2)} = \frac{(\gamma-1)\,\omega_1^2}{4\,\gamma}\left[n^2 + 2\,i\,(n+i)\right].$$

This system of equations has the form of a system of nonlinearly coupled oscillators. The parameters α_n and θ_n account for the linear processes mentioned above and represent the linear damping and frequency shift of each mode respectively. Parameter values used in this study were obtained from Paparizos and Culick[1] and are listed in Table I.

Previous analysis of this system has concentrated on the time averaged equations for two modes only.The system was truncated at two modes because it has not yet been possible to obtain literal solutions for more than two modes.Analytically determining the existence and stability of thelimit cycles of a fourth-order system is still a difficult problem so time averaging was applied to the set (1.1). Time averaging and a coordinate transformation (see Section 3.1) changes the problem to one of determining the steady states of a third-order system, a problem that can be solved analytically. Paprizos and Culick[1] carried out time simulations for systems of up to ten modes and, as expected, discovered differences related to the number of modes included in the truncated system. The present analysis uses dynamical systems theory and continuation techniques to study the effects of time averaging and truncation at a small number of modes on the limit cycle behavior of the system.

It is helpful to nondimensionalize time by the fundamental acoustic frequency, ω_1, so events occur on a time scale of one. Applying the transformation

$$t = \tfrac{1}{\omega_1}\,\hat{t}, \tag{1.2}$$

where $\hat{t}$ is nondimensional time, results in the system

$$\omega_1^2\,\ddot{\eta}_n + \omega_n^2\,\eta_n = 2\,\alpha_n\,\omega_1\,\dot{\eta}_n + 2\,\theta_n\,\omega_n\,\eta_n - \sum_{i=1}^{n-1}\left(\omega_1^2\,C_{ni}^{(1)}\,\dot{\eta}_i\,\dot{\eta}_{n-i} + D_{ni}^{(1)}\,\eta_i\,\eta_{n-i}\right) - 2\sum_{i=1}^{\infty}\left(\omega_1^2\,C_{ni}^{(2)}\,\dot{\eta}_i\,\dot{\eta}_{n+i} + D_{ni}^{(2)}\,\eta_i\,\eta_{n+i}\right). \tag{1.3}$$

Since this study is restricted to longitudinal acoustic modes in a cylindrical combustion chamber the modal frequencies are related by the equation

$$\omega_n = n\,\omega_1. \tag{1.4}$$

Substituting this relation into Equation (1.3) results in the system

$$\ddot{\eta}_n + n^2\,\eta_n = 2\,\hat{\alpha}_n\,\dot{\eta}_n + 2\,n\hat{\theta}_n\,\eta_n - \sum_{i=1}^{n-1}\left(C_{ni}^{(1)}\,\dot{\eta}_i\,\dot{\eta}_{n-i} + \frac{1}{\omega_1^2}\,D_{ni}^{(1)}\,\eta_i\,\eta_{n-i}\right) - 2\sum_{i=1}^{\infty}\left(C_{ni}^{(2)}\,\dot{\eta}_i\,\dot{\eta}_{n+i} + \frac{1}{\omega_1^2}\,D_{ni}^{(2)}\,\eta_i\,\eta_{n+i}\right) \tag{1.5}$$

where

$$\hat{\alpha}_n = \frac{\alpha_n}{\omega_1}$$
$$\hat{\theta}_n = \frac{\theta_n}{\omega_1}.$$

To analyze Equation (1.5) with techniques from dynamical systems theory and continuation methods it must be written as a first-order system. This can be done by defining the new variable

$$\xi_n = \dot{\eta}_n. \tag{1.6}$$

The system then has the form

$$\dot{\eta}_n = \xi_n$$
$$\dot{\xi}_n = -n(n - 2\,\hat{\theta}_n)\eta_n + 2\,\hat{\alpha}_n\,\xi_n - \sum_{i=1}^{n-1}\left(\hat{C}_{ni}^{(1)}\,\xi_i\,\xi_{n-i} + \hat{D}_{ni}^{(1)}\,\eta_i\,\eta_{n-i}\right) - \sum_{i=1}^{\infty}\left(\hat{C}_{ni}^{(2)}\,\xi_i\,\xi_{n+i} + \hat{D}_{ni}^{(2)}\,\eta_i\,\eta_{n+i}\right) \tag{1.7}$$

where

$$\hat{C}_{ni}^{(1)} = \frac{-1}{2\,\gamma\,i\,(n-i)}\left[n^2 + i\,(n-i)(\gamma-1)\right]$$
$$\hat{C}_{ni}^{(2)} = \frac{1}{\gamma\,i\,(n+i)}\left[n^2 - i\,(n+i)(\gamma-1)\right]$$
$$\hat{D}_{ni}^{(1)} = \frac{\gamma-1}{4\,\gamma}\left[n^2 - 2\,i\,(n-i)\right]$$
$$\hat{D}_{ni}^{(2)} = \frac{\gamma-1}{2\,\gamma}\left[n^2 + 2\,i\,(n+i)\right].$$

Time averaging is applied to Equation (1.7) by assuming that the time dependent amplitude of each acoustic mode has the form

$$\eta_n(\hat{t}) = A_n(\hat{t})\ \sin(n\hat{t}) + B_n(\hat{t})\ \cos(n\hat{t}). \quad (1.8)$$

Substituting Equation (1.8) into Equation (1.7) and averaging the resulting system over the period ($0 \rightarrow 2\pi$) results in the system (Paparizos and Culick[1])

$$\begin{aligned}\dot{A}_n &= \hat{\alpha}_n A_n + \hat{\theta}_n B_n \\ &\quad + \frac{1}{2} n \kappa \sum_{i=1}^{n-1} \Big[A_i A_{n-i} - B_i B_{n-i} \Big] \\ &\quad - n \kappa \sum_{i=1}^{\infty} \Big[A_{n+i} A_i + B_{n+i} B_i \Big] \\ \dot{B}_n &= \hat{\alpha}_n B_n - \hat{\theta}_n A_n \\ &\quad + \frac{1}{2} n \kappa \sum_{i=1}^{n-1} \Big[A_i B_{n-i} + B_i A_{n-i} \Big] \\ &\quad + n \kappa \sum_{i=1}^{\infty} \Big[A_{n+i} B_i - B_{n+i} A_i \Big]\end{aligned} \quad (1.9)$$

where

$$\kappa = \frac{\gamma + 1}{8\,\gamma}.$$

Steady states of Equation (1.9) represent limit cycles of the time dependent amplitudes of the acoustic modes, η_n, because of the time dependence specified by Equation (1.8).

The zero solution of Equation (1.9) ($A_n = B_n = 0$) represents a zero pressure perturbation of the original system. The stability of this steady state is given by the eigenvalues of the linearized system,

$$\lambda_n = \hat{\alpha}_n \pm \mathbf{i}\,\hat{\theta}_n.$$

Thus, when $\hat{\alpha}_n$ is zero this system undergoes a Hopf bifurcation. As discussed previously, Hopf bifurcations lead to the existence of limit cycles, so when $\hat{\alpha}_n$ is positive Equation (1.9) will undergo limit cycle behavior. This seems to suggest that time averaging did not really make the continuation problem any easier because the time averaged system also contains limit cycles. Thus, when applying the continuation method to the time averaged system it is necessary to continue a limit cycle as opposed to a steady state. This is an important distinction because the computer time required to determine the limit cycles of a system with continuation methods is several orders of magnitude longer than the computer time required to determine the steady states of the system. Time averaging does reduce the computational time required to do numerical simulations because the high frequency content of the pressure fluctuation is eliminated by time averaging, making it possible to use larger time steps in the simulation.

Applying time averaging to Equation (1.7) did not convert the limit cycles of Equation (1.7) to steady states of Equation (1.9) because the van der Pol transformation applied before time averaging [Equation (1.8)] did not use the proper frequency in the sine and cosine terms. The eigenvalues of the system obtained by linearizing Equation (1.7) about the origin were shown to be

$$\lambda_n = \hat{\alpha}_n \pm \mathbf{i}\, n \sqrt{1 - (2\,\hat{\theta}_n/n) - (\hat{\alpha}_n/n)^2}$$

so the van der Pol transformation should have had the form

$$\eta_n(\hat{t}) = A_n(\hat{t})\ \sin(\Omega_n\,\hat{t}) + B_n(\hat{t})\ \cos(\Omega_n\,\hat{t}) \quad (1.10)$$

where

$$\Omega_n = n \sqrt{1 - (2\,\hat{\theta}_n/n) - (\hat{\alpha}_n/n)^2}.$$

It is not possible to apply time averaging with this van der Pol transformation because the frequencies, Ω_n, are not integral multiples of each other. Thus in the linear approximation, the frequencies of the time dependent amplitudes of the acoustic modes are not integer multiples of each other. A limit cycle of a given frequency will exist for the complete system through the interaction of the nonlinear terms, but it is not possible to calculate this frequency analytically.

Since Equation (1.9) is expected to contain limit cycles as asymptotic motions it is useful to transform Equation (1.9) into polar coordinates. This can be accomplished by defining the coordinate transformation

$$\begin{aligned}A_n &= r_n\ \cos\phi_n \\ B_n &= r_n\ \sin\phi_n.\end{aligned} \quad (1.11)$$

Taking the time derivative of Equation (1.11),

$$\begin{pmatrix} \dot{r}_n \\ \dot{\phi}_n \end{pmatrix} = \begin{pmatrix} \cos\phi_n & \sin\phi_n \\ -\frac{1}{r}\sin\phi_n & \frac{1}{r}\cos\phi_n \end{pmatrix} \begin{pmatrix} \dot{A}_n \\ \dot{B}_n \end{pmatrix}, \quad (1.12)$$

and applying this transformation to Equation (1.9) results in the system

$$\begin{aligned}\dot{r}_n &= \\ &\hat{\alpha}_n\, r_n + \frac{1}{2} n\kappa \sum_{i=1}^{n-1} r_i\, r_{n-i}\ \cos(\phi_i + \phi_{n-i} - \phi_n) \\ &- n\,\kappa \sum_{i=1}^{\infty} r_i\, r_{n+i}\ \cos(\phi_i + \phi_n - \phi_{n+i}) \\ \dot{\phi}_n &= \\ &- \hat{\theta}_n + \frac{1}{2} n\kappa \sum_{i=1}^{n-1} \left(\frac{r_i\, r_{n-i}}{r_n} \right) \sin(\phi_i + \phi_{n-i} - \phi_n) \\ &+ n\,\kappa \sum_{i=1}^{\infty} \left(\frac{r_i\, r_{n+i}}{r_n} \right) \sin(\phi_i + \phi_n - \phi_{n+i}).\end{aligned} \quad (1.13)$$

Paparizos and Culick[1] have shown that in the limit cycle one would expect the frequencies of the time dependent amplitudes of the acoustic modes ($\omega_n - n\,\phi_n(\hat{t})$) to be integer multiples of each other. Since $\omega_n = n\,\omega_1$ for the case considered here, one might expect

$$\frac{d}{dt}\Big(\phi_n(t) - n\,\phi_1(t)\Big) = 0$$

in the limit cycle. With this in mind it seems useful to replace the variables ϕ_n by the new variable

$$\psi_n = n\,\phi_1 - \phi_n.$$

Substituting this new variable into Equation (1.13) results in the system

$$\begin{aligned}
\dot{r}_n = &\\
&\widehat{\alpha}_n\, r_n + \frac{1}{2} n\,\kappa \sum_{i=1}^{n-1} r_i\, r_{n-i}\, \cos(\psi_n - \psi_{n-i} - \psi_i)\\
&- n\,\kappa \sum_{i=1}^{\infty} r_i\, r_{n+i}\, \cos(\psi_{n+i} - \psi_n - \psi_i)\\
&\qquad\qquad\qquad\qquad n = 1, \ldots, N\\
\dot{\psi}_n = &(\widehat{\theta}_n - n\widehat{\theta}_1)\\
&- \frac{1}{2}\, n\,\kappa \sum_{i=1}^{n-1} \left(\frac{r_i\, r_{n-i}}{r_n}\right) \sin(\psi_n - \psi_{n-i} - \psi_i)\\
&- n\,\kappa \sum_{i=1}^{\infty} \left(\frac{r_i\, r_{n+i}}{r_n}\right) \sin(\psi_{n+i} - \psi_n - \psi_i)\\
&+ n\,\kappa \sum_{i=1}^{\infty} \left(\frac{r_i\, r_{i+1}}{r_1}\right) \sin(\psi_{i+1} - \psi_i)\\
&\qquad\qquad\qquad\qquad n = 2, \ldots, N.
\end{aligned} \tag{1.14}$$

Note that ψ_1 is zero by definition, so the dimension of the system has been reduced from $2N$ to $2N-1$. This reduction in the order of the system is possible because the reference value of the phase is arbitrary; the important quantity is the difference between the phases of the various modes. Thus, one can define all phases relative to the phase of mode one as was done above.

II. Theoretical Background

2.1 Dynamical Systems Theory

Dynamical systems theory is a methodology for studying systems of ordinary differential equations. Many systems have been studied using dynamical systems theory but it has not been used to study nonlinear acoustics in combustion chambers. The important ideas of dynamical systems theory used in this report will be introduced in the following paragraphs. More information can be found in the book of Guckenheimer and Holmes[2].

The first step in analyzing a system of nonlinear differential equations, in the dynamical systems theory approach, is to calculate the steady states of the system and their stability. Steady states can be determined by setting all time derivatives equal to zero and solving the resulting set of algebraic equations. The Hartman-Grobman Theorem [Guckenheimer and Holmes[2], Chapter 1, page 13] proves that the local stability of a steady state can be determined by linearizing the equations of motion about the steady state and calculating the eigenvalues. A steady state is linearly stable if the real parts of the eigenvalues are negative and linearly unstable if any eigenvalue has a positive real part. In the neighborhood of a steady state (i.e. a region where the linear analysis is valid) the sytem will be attracted to the steady state if it is stable and repelled from it if the steady state is unstable.

The Implicit Function Theorem [Ioos and Joseph[3], Chapter 2, pages 13–14] proves that the steady states of a system are continuous functions of the parameters of the system. Thus, the steady states on the nonlinear acoustic equations are continuous functions of the linear stability parameters of each mode, α_n. Stability changes can occur as the parameters of the system are varied in such a way that the real parts of one or more eigenvalues of the linearized system change sign. Changes in the stability of a steady state lead to qualitatively different responses for the system and are called bifurcations. Stability boundaries can be determined by searching for steady states which have one or more eigenvalues with zero real parts.

There are many types of bifurcations and each type has a different effect on the response of the system. Qualitative changes in the response of the system can be predicted by determining how many and what type of eigenvalues have zero real parts at the bifurcation point. Bifurcations for which one real eigenvalue is zero lead to the creation or destruction of two or more steady states. Bifurcations for which one pair of imaginary eigenvalues has zero real parts can lead to the creation or destruction of periodic motions. Bifurcations for which more than one real eigenvalue or more than one pair of complex eigenvalues has zero real parts lead to very complicated behavior and are beyond the scope of this report.

Results presented in this report will also be concerned with the limit cycle behavior of dynamical systems. In particular, the pressure oscillations referred to as combustion instabilities in combustion systems are represented by limit cycles of the amplitude equations. Limit cyles can undergo bifurcations similiar to the bifurcations of steady states discussed above. Analytical results generally involve the study of the Poincare map of the system. Bifurcations of limit cycles occur when one or more eigenvalues of the linearized map about the limit cycle have a magnitude equal to one.

One real eigenvalue equal to positive one signifies a pitchfork bifurcation, one real eigenvalue equal to negative one signifies a period doubling bifurcation, and one complex eigenvalue with magnitude equal to one signifies a Hopf bifurcation of the limit cycle. A thorough discussion of the various types of bifurcations of both steady states and limit cycles that can occur in a dynamical system is given in Guckenheimer and Holmes[2].

2.2 Continuation of Steady States

Continuation methods are a direct result of the Implict function theorem, which proves that the steady states of a system are continuous functions of the parameters of the system. The general technique is to fix all parameters of the system but one and trace the steady states of the system as a function of this parameter. For a system of ordinary differential equations of the form

$$\dot{x} = f(x;\mu), \tag{2.1}$$

where x is a vector representing the state of the system and μ is a one-dimensional parameter, the implict function theorem proves that the steady states of the system are continuous functions of the parameter, μ. Thus, solutions of the equation

$$f(x;\mu) = 0, \tag{2.2}$$

are continuous functions of μ. Continuation methods are numerical techniques for calculating solutions of Equation (2.2).

The technique used in this work is called a pseudo arc-length continuation technique and is from Doedel and Kernevez[4]. In this numerical technique the parameter, μ, is treated as an unknown along with x and x and μ are calculated as functions of arc length, s, along the curve of steady states. If one steady state of the system is known, a new steady state can be approximated by linear extrapolation from the known steady state (see Figure 1). The slope of the curve at the known steady state can be determined by taking the derivative of Equation (2.2) with respect to s,

$$f_x\, x' + f_\mu\, \mu' = 0, \tag{2.3}$$

where,

$$\begin{aligned} x' &= \frac{dx}{ds} \\ \mu' &= \frac{d\mu}{ds}, \end{aligned} \tag{2.4}$$

and solving for x' and μ'. The change in x and μ in one step along the curve is limited by normalizing x' and μ' with the relation

$$(x')^2 + (\mu')^2 = 1. \tag{2.5}$$

The error between the approximate steady state and the true steady is then reduced to an acceptable level with Newton's method.

The above technique is computationally expensive as it is necessary to invert the matrix (f_x, f_μ) to solve for x' and μ' at each step. If two steady states of Equation (2.1), (x_0, μ_0) and (x_1, μ_1), are known, an approximation to the above technique can be used. This involves approximating Equation (2.5) with the pseudo arc-length continuation equation

$$(x - x_1)\, x_1' + (\mu - \mu_1)\, \mu_1' - \Delta s = 0, \tag{2.6}$$

where Δs is the step size along the solution curve and x_1' and μ_1' are the values of x' and μ' evaluated at (x_1, μ_1). The values of x_1' and $\mu_1\prime$ can be approximated by (see Figure 2)

$$\begin{aligned} x_1' &= \frac{(x_1 - x_0)}{\Delta s}, \\ \mu_1' &= \frac{(\mu_1 - \mu_0)}{\Delta s}. \end{aligned} \tag{2.7}$$

Steady states of Equation (2.1) are then calculated by solving

$$\begin{aligned} f(x;\mu) &= 0, \\ (x - x_1)\, x_1' + (\mu - \mu_1)\, \mu_1' - \Delta s &= 0, \end{aligned} \tag{2.8}$$

with the following algorithm:

(1) Approximate x_1' and μ_1' at the known steady state,
(2) Approximate the unknown steady state; $x = x_1 + x_1' \Delta s$, $\mu = \mu_1 + \mu_1' \Delta s$,
(3) Use Newton's method to reduce the error between the approximate and true steady state to an acceptable level.

2.3 Continuation of Limit Cycles

To study combustion instabilities it is also necessary to compute the limit cycles of a dynamical system. It is possible to compute the limit cycles of a dynamical system by discretizing the system in time and turning the computation of limit cycles into a calculation of steady states. More specifically, periodic orbits of Equation (2.1) are given by solutions of

$$\begin{aligned} \dot{x} - f(x(t);\mu) &= 0 \\ x(0) - x(\tau) &= 0 \end{aligned} \tag{2.9}$$

where τ is the period of the limit cycle. Scaling time by the relation $t \mapsto \frac{t}{\tau}$ transforms Equation (2.9) into

$$\begin{aligned} \dot{x} - \tau\, f(x(t);\mu) &= 0, \\ x(0) - x(1) &= 0. \end{aligned} \tag{2.10}$$

All periodic orbits of Equation (2.10) have a period equal to one. Using the techniques discussed above for steady states, μ will be treated as an unknown and solutions will be calculated as a function of arc length, s, along the curve of limit cycles. Since the period of the limit cycle of Equation (2.9), τ, is unknown another equation is needed to make the system solvable. The extra equation can be derived by noting that two periodic orbits at subsequent values of arc length, s, have an arbitrary phase difference. This is true because if $x(t)$ is a periodic orbit satasfying Equation (2.10), then $x(t+\sigma)$ is also a periodic orbit satisfying Equation (2.10). Thus, if $x_k(t)$ is a known periodic orbit of Equation (2.10) and $x(t)$ is the subsequent unknown periodic orbit of Equation (2.10), the arbitrary phase difference between the periodic orbits can be eliminated by minimizing (Doedel and Kernevez[4])

$$g(\sigma) = \int_0^1 ||x(t+\sigma) - x_k(t)||_2^2 \, dt. \tag{2.11}$$

Equating the derivative of Equation (2.11) to zero results in the equation

$$\int_0^1 \Big(\widetilde{x}(t) - x_k(t)\Big)\, \dot{\widetilde{x}}(t)\, dt = 0, \tag{2.12}$$

where $\widetilde{x}(t) = x(t+\widehat{\sigma})$ and $\widehat{\sigma}$ denotes the value of σ that minimizes Equation (2.11). Integrating Equation (2.12) by parts gives the phase condition

$$\int_0^1 \widetilde{x}(t)\, \dot{x}_k(t)\, dt = 0, \tag{2.13}$$

which will be used in the continuation technique. Note that $\widetilde{x}(0) = \widetilde{x}(1)$ and $x_k(0) = x_k(1)$ as a result of the periodicity of the solutions.

The pseudo arc-length continuation equation used for calculating the steady states of a dynamical system, Equation (2.6). will have to be generalized to calculate the limit cycle of a dynamical system. The change is necessary because the solution is now a function of time. Time dependence of the solution can be accounted for by calculating the quantities represented by Equation (2.6) over one period of the limit cycle,

$$\int_0^1 \Big(x(t) - x_k(t)\Big)\, x_k'(t)\, dt + (\mu - \mu_k)\, \mu_k' + (\tau - \tau_k)\, \tau_k' - \Delta s = 0. \tag{2.14}$$

The complete system for calculating the $(k+1)^{st}$ limit cycle of Equation (2.1), $\big(x(t), \mu, \tau\big)$, when the k^{th} limit cycle is known is

$$F\big(x(t); \mu, \tau\big) = \begin{pmatrix} \dot{x} - \tau\, f\big(x(t); \mu\big) \\ x(0) - x(1) \\ \int_0^1 x(t)\, \dot{x}_k(t)\, dt \\ \int_0^1 \big(x(t) - x_k(t)\big)\, x_k'(t)\, dt \\ +(\mu - \mu_k)\, \mu_k' + (\tau - \tau_k)\, \tau_k' - \delta s \end{pmatrix} = 0. \tag{2.15}$$

Periodic orbits of Equation (2.1) are functions of time, $x(t)$, that satisfy Equation (2.15). It is exceedingly difficult if not impossile to analytically or computationally determine the functions $x(t)$ that satisfy these equations. One way of solving this system is to discretize the periodic orbit, $x(t)$, in time. In particular, divide the period $0 \le t \le 1$, into N intervals. In the jth interval define the Lagrange basis polynomial

$$a_{j,i}(t) = \prod_{k=0, k\neq i}^{m} \frac{t - (t_j + \frac{k}{m}\Delta t)}{\frac{(i-k)}{m}\Delta t}, \tag{2.16}$$

and approximate the periodic orbit, $x(t)$, in the jth interval by

$$x_j(t) = \sum_{i=0}^{m} a_{j,i}(t) u_{j+i/m}. \tag{2.17}$$

The key characteristic of the basis polynomials, $a_{j,i}(t)$, is that

$$\begin{aligned} a_{j,i}(t_j + \frac{i}{m}\Delta t) &= 1 \\ a_{j,i}(t_j + \frac{k}{m}\Delta t) &= 0; \quad k \neq i. \end{aligned} \tag{2.18}$$

Thus,

$$x_j\big(t_j + \frac{i}{m}\Delta t\big) = u_{j+i/m} \tag{2.19}$$

and $u_{j+i/m}$ represents the discrete approximation of the periodic solution $x(t)$ at time, $t = t_j + \frac{i}{m}\Delta t$.

The method then consists of solving

$$\dot{x}_j(z_{j,i}) - \tau\, f\Big(x_j(z_{j,i}); \mu\Big) = 0, \tag{2.20}$$

for $i = 1, \ldots, m$ and $j = 1, \ldots, N$, where $z_{j,i}$ are the zeroes of the m^{th} degree Legendre polynomial relative to the appropriate subinterval. By discretizing the equation in this manner, the new unknowns are the $u_{j+i/m}$. This technique is a generalization of relaxation methods (Press, *et al.*[5], p. 609), in which ordinary differential equations are approximated by finite difference equations on a grid or mesh over the domain. By using Lagrange basis polynomials to supply the time dependence and then solving the system at discrete values of time, the time dependence is removed from the system of equations to be solved.

The integral equations in Equation (2.15) are discretized by a composite quadrature formula obtained by approximate integration over each subinterval of time (Press *et al.*[5], page 131). Gauss-Legendre quadratures are used in this work so the collocation points, $z_{j,i}$ at which Equation (2.15) is solved were chosen as the zeroes of the m^{th} degree Legendre polynomial relative to the appropriate subinterval. This choice of collocation points allows one to easily handle integral equations included in the dynamical system.

The problem is then one of finding the steady states of a system of ordinary differential equations where the new variables are the $u_{j+i/m}$. This is much easier than finding the periodic orbits of Equation (2.1), and one that can be solved with the continuation algorithm discussed above, but this simplification comes at a price. Discretizing the system results in a large increase in the dimension of the system to be solved. In particular, if the dimension of the original system, Equation (2.1), is n, then Equation (2.15) has dimension $2n + n$. Now suppose the system is discretized into N time intervals with m collocation points in each subinterval. The dimension of the discretized system will then be $Nmn+n+2$, which can be very large.

The stability of the periodic orbits is determined by calculating the Floquet multipliers of the discretized system (Guckenheimer and Holmes[2], page 24). Floquet multipliers of the periodic orbits are analogous to the eigenvalues of a steady state. The basic technique is to linearize the system of equations [in our case Equation (2.1)] about the periodic orbit and calculate the solution of the linearized equations. This is not a trivial matter because you first need to determine the periodic orbit. An alternate technique is to calculate the eigenvalues of the linearized Poincare map, which are equivalent to the Floquet multipliers. In the present work, an approximation to the linearized Poincare map is used to calculate the Floquet multipliers of the orbit (Doedel and Kernevez[4], page 44).

Bifurcations can be found by searching for periodic orbits that have one or more Floquet multipliers whose magnitude is one. A purely real Floquet multiplier equal to positive one would signify a pitchfork bifurcation, while a purely real Floquet multiplier equal to negative one would signify a period doubling bifurcation. A pair of complex Floquet multipliers whose magnitude is equal to one would signify a Hopf bifurcation of the Poincare map of the system a lead to the appearance of quasi-periodic motions (i.e. flow on a torus). These are commonly called torus bifurcations.

III. Analysis of Steady States

The steady states of Equation (1.7) are determined by setting the time derivatives equal to zero ($\dot{\eta}_n = \dot{\xi}_n = 0$) and solving the resulting algebraic equations. It is easy to see that the zero solution, (η_n, ξ_n)=(0,0), is a steady state for equation (1.7) no matter how many modes are included in the system. This steady state corresponds to zero pressure perturbation in the combustion chamber and is the steady state of interest in this study.

The stability of the zero steady state can be determined by calculating the eigenvalues of the system obtained by linearizing Equation (1.7) about the origin. Linearizing Equation (1.7) about the origin gives

$$\begin{pmatrix} \dot{\eta}_n \\ \dot{\xi}_n \end{pmatrix} = \begin{pmatrix} 0 & 1 \\ -(n^2 - 2\,n\,\widehat{\theta}_n) & 2\,\widehat{\alpha}_n \end{pmatrix} \begin{pmatrix} \eta_n \\ \xi_n \end{pmatrix}. \quad (3.1)$$

Note that the acoustic modes represented by Equation (1.7) are linearly uncoupled, so the linearized system for an N-mode approximation will consist of N pairs of linear, uncoupled equations. It is thus possible to determine the eigenvalues of the linearized system independent of the number of modes included in the approximation. If the acoustic modes were linearly coupled, the eigenvalues for each mode would in general depend on the number of modes included in the approximation. The eigenvalues of the n^{th} mode are

$$\lambda_n = \widehat{\alpha}_n \pm \mathbf{i}\, n \sqrt{1 - (2\,\widehat{\theta}_n/n) - (\widehat{\alpha}_n/n)^2}. \quad (3.2)$$

If $\widehat{\alpha}_n$ is zero, then the eigenvalues of the n^{th} mode are pure imaginary and a Hopf bifurcation occurs. This leads to the existence of limit cycles when $\widehat{\alpha}_n$ is positive for one or more modes. These limit cycles represent time vary amplitudes of the acoustic modes and are physically realized as combustion instabilities.

Equation (1.7) has steady states besides the steady state at the origin. A pair of nonzero steady states can be analytically determined for the two mode approximation, but they are physically unrealistic as they are greater than one. In particular, for $\gamma = 1.4$, the steady states are given by $(\eta_1, \eta_2) = (\pm 6.3, 1.4)$ (Jahnke[6]). These steady states are unstable so they will not affect the dynamics of the system near the origin. It is important to determine all the steady states of a system and their stability to obtain a full understanding of the system. If a steady state is stable, the system may be attracted to that steady state whether or not the steady state is physically realistic.

Steady states other than the zero steady state were also found for the four- and six-mode approximations. These steady states were found using a continuation algorithm as it was impossible

to determine the steady states analytically. Four nonzero steady states were found for the four-mode approximation. All these steady states were physically unrealistic and linearly unstable, so they will not affect the dynamics of the system. Six nonzero steady states were found for the six-mode approximation; these were also physically unrealistic and linearly unstable.

IV. Results for a First-Mode Instability

4.1 Two-Mode Time-Averaged Equations

The two-mode time-averaged equations in polar coordinates can be obtained from Equation (1.13) to give the system of first-order ordinary differential equations

$$\begin{aligned}
\dot{r}_1 &= \widehat{\alpha}_1 r_1 - \kappa r_1 r_2 \cos(2\phi_1 - \phi_2) \\
\dot{\phi}_1 &= -\widehat{\theta}_1 + \kappa r_2 \sin(2\phi_1 - \phi_2) \\
\dot{r}_2 &= \widehat{\alpha}_2 r_2 + \kappa r_1^2 \cos(2\phi_1 - \phi_2) \\
\dot{\phi}_2 &= -\widehat{\theta}_2 + \kappa \left(\frac{r_1^2}{r_2}\right) \sin(2\phi_1 - \phi_2).
\end{aligned} \tag{4.1}$$

The angular variables ϕ_1 and ϕ_2 only appear in Equation (4.1) in the combination $2\phi_1 - \phi_2$, which equals ψ_2 by definition (see Section I). Based on this observation or by using Equation (1.14), Equation (4.1) can be written as the third-order system

$$\begin{aligned}
\dot{r}_1 &= \widehat{\alpha}_1 r_1 - \kappa r_1 r_2 \cos\psi_2 \\
\dot{r}_2 &= \widehat{\alpha}_2 r_2 + \kappa r_1^2 \cos\psi_2 \\
\dot{\psi}_2 &= (\widehat{\theta}_2 - 2\widehat{\theta}_1) + \kappa\left(2r_2 - \frac{r_1^2}{r_2}\right) \sin\psi_2.
\end{aligned} \tag{4.2}$$

Paparizos and Culick[1] derived an equivalent form of the two-mode time-averaged equations using the transformation

$$\begin{aligned}
A_n &= r_n \sin(\phi_n - n\phi_1) \\
B_n &= r_n \cos(\phi_n - n\phi_1)
\end{aligned} \tag{4.3}$$

in place of the transformation given by Equation (1.11). Paparizos and Culick[1] then went on to show that stable steady states of the two-mode time-averaged equations only exist if $\widehat{\alpha}_2/\widehat{\alpha}_1 < -2$ and that the steady states are given by

$$\begin{aligned}
r_1 &= \frac{1}{\kappa}\sqrt{-\widehat{\alpha}_1 \widehat{\alpha}_2 (1+\beta^2)} \\
r_2 &= \frac{1}{\kappa}\sqrt{\widehat{\alpha}_1^2 (1+\beta^2)} \\
\psi_2 &= \tan^{-1}(-\beta)
\end{aligned} \tag{4.4}$$

where

$$\beta = \frac{\widehat{\theta}_2 - 2\widehat{\theta}_1}{2\widehat{\alpha}_1 + \widehat{\alpha}_2}.$$

It is important to note that the steady state of Equation (4.2) does not necessarily represent a steady state of the two-mode time-averaged equations, Equation (4.1). The condition that $\dot{\psi}_2$ equals zero means that $2\dot{\phi}_1 - \dot{\phi}_2$ equals zero but not necessarily that $\dot{\phi}_1$ and $\dot{\phi}_2$ are individually equal to zero. It is easy to solve for the time dependence of ϕ_1 and ϕ_2 by substituting the steady state values of r_1 and r_2 into Equation (4.1). This shows that at the stead state values of r_1 and r_2,

$$\begin{aligned}
\dot{\phi}_1 &= -\left(\frac{\widehat{\alpha}_1 \widehat{\theta}_2 + \widehat{\alpha}_2 \widehat{\theta}_1}{2\widehat{\alpha}_1 - \widehat{\alpha}_2}\right) \\
\dot{\phi}_2 &= -2\left(\frac{\widehat{\alpha}_1 \widehat{\theta}_2 + \widehat{\alpha}_2 \widehat{\theta}_1}{2\widehat{\alpha}_1 - \widehat{\alpha}_2}\right)
\end{aligned} \tag{4.5}$$

so the steady states of Equation (4.2) represent limit cycles of the two-mode time-averaged equations, Equation (4.1). The solution of the two-mode time-averaged approximation to the nonlinear acoustics in a cylindrical combustion chamber is thus given by

$$\begin{aligned}
&\eta_1(t) = \\
&\quad \frac{8\gamma}{(\gamma+1)\omega_1}\sqrt{-\alpha_1 \alpha_2 (1+\beta^2)}\sin(\omega_1 t + \phi_1(t)) \\
&\eta_2(t) = \\
&\quad \frac{8\gamma}{(\gamma+1)\omega_1}\sqrt{\alpha_1^2 (1+\beta^2)}\sin(2\omega_1 t + \phi_2(t))
\end{aligned} \tag{4.6}$$

where

$$\begin{aligned}
\phi_1(t) &= -\left(\frac{\alpha_1 \theta_2 + \alpha_2 \theta_1}{2\alpha_1 - \alpha_2}\right) t + \phi_{10} \\
\phi_2(t) &= -2\left(\frac{\alpha_1 \theta_2 + \alpha_2 \theta_1}{2\alpha_1 - \alpha_2}\right) t + \phi_{20} \\
\beta &= \left(\frac{\theta_2 - 2\theta_1}{\alpha_2 + 2\alpha_1}\right)
\end{aligned}$$

and

$$2\phi_{10} - \phi_{20} = \tan^{-1}(-\beta).$$

Note that the time dependence of ϕ_1 and ϕ_2 changes the frequency of the time dependent amplitude of the acoustic mode.

The maximum amplitudes of $\eta_1(t)$ and $\eta_2(t)$ in the limit cycle are shown in Figure 3 as functions of α_1/α_2. Figure 3 shows that a limit cycle exists when α_1/α_2 is negative, but is stable only if α_1/α_2 is less than negative 1/2. It is important to note that the amplitude of the limit cycle goes to infinity as α_1/α_2 approaches $-1/2$, which coincides with the stability boundary of the limit cycle. Since the original equations representing the time evolution of the amplitudes of the acoustic modes were derived using a perturbation analysis, only limit cycles with small amplitudes are valid approximations to solutions of the complete fluid dynamic equations. Also, time averaging is

theoretically valid only if the amplitudes in the limit cycle remain small. Thus one would expect that the limit cycles predicted by the two-mode time-averaged equations are not valid for values of α_1/α_2 near $-1/2$. It is particularly important to take this into account when considering the validity of the stability boundary predicted by the two-mode time-averaged equations.

4.2 Two-Mode Continuation Results

Time averaging clearly simplifies the analysis of the two-mode approximation, but this simplification comes at cost. In order to apply time averaging, a sinusoidal time dependence is explicitly specified for each acoustic mode. This fixes the period of the limit cycle and makes it possible to integrate over one period. These approximations are valid near the Hopf bifurcation point (i.e. for $\widehat{\alpha}_1 << 1$), but as $\widehat{\alpha}_1$ becomes larger the approximation becomes less and less valid.

Continuation methods make it possible to compute the limit cycles of Equation (1.7) as a function of one of the parameters of the system without resorting to time averaging. In this section, the continuation technique is used to determine the existence and stability of limit cycles of Equation (1.7) as a function of the linear damping parameter of the fundamental acoustic mode, α_1. Limit cycles of Equation (1.7) will exist as a result of the Hopf bifurcation that occurs when α_1 is zero. This Hopf bifurcation point is used as the starting point for the continuation method. Figure 4 shows the results obtained by applying the continuation method to the two-mode approximation. The maximum amplitudes of the first and second acoustic modes in the limit cycle are plotted as functions of α_1, along with the period of the limit cycle, τ, and the maximum amplitude of the pressure fluctuation at the head of the combustion chamber, $P'(x = 0, t)$. The maximum ampitude of the pressure fluctuation at the head of the combuation chamber is used as a measure of the validity of the perturbation equations. Results in which the pressure perturbation is greater than one half of the mean chamber pressure are probably not valid. The stability of the limit cycle is also indicated in Figure 4; stable limit cycles are represented by solid lines while unstable limit cycles are represented by dashed lines.

Results from the time-averaged equations are also plotted in Figure 4 to show the differences between the results obtained by the continuation method and the results obtained by time averaging. Results from the two methods are practically the same for values of α_1 less than 120. Note that the change in the period of the limit cycle as a function of α_1 is poorly approximated by the time-averaged equations. Recall that the change in the period of the limit cycle predicted by the time-averaged equations occurs because the asymptotic motion of the time-averaged equation is a limit cycle.

The limit cycle behaviors predicted by the continuation method and the time-averaged equations are significantly different for values of α_1 greater than 120. The continuation method predicts that a turning point bifurcation occurs for α_1 equal to 131, beyond which no limit cycle will exist. The limit cycle also becomes asymmetric near the turning point. This is particularly evident in the plot of the pressure perturbation at the head of the combustion chamber. The limit cycle behavior predicted by the time-averaged equations remains symmetric by definition. Also note that the amplitude of the pressure perturbation at the turning point is close to one-half of the mean chamber pressure so the perturbation expansion used to obtain the acoustic equations may not be valid.

4.3 Four-Mode Time Averaged Results

The four-mode time-averaged equations are obtained by using Equation (1.9) for $n = 1, 2, 3, 4$. Recall from the previous discussion that the asymptotic motion of the time-averaged equations is a limit cycle arising from the Hopf bifurcation that occurs when α_1 equals zero. For the two-mode case, it was possible to turn the problem from one of determining the limit cycles of a fourth-order system to one of determining the steady states of a third-order system by noting that the phases of the time dependent amplitudes, ϕ_1 and ϕ_2, only occur in the combination $2\phi_1 - \phi_2$. States of the resulting third-order system could then be determined analytically.

By using Equation (1.14) to obtain the time-averaged equations for the four-mode approximation in polar coordinates, one obtains a seventh-order system. It is not possible to determine the steady states of this system analytically, however it should be possible to determine them using a continuation method. This has not been accomplished at this point, but should be in the near future. The main difficulty is that the equations are singular when any r_n are zero, which is exactly the value of r_n at the Hopf bifurcation, where one would expect the nonzero steady states of the averaged system to initially appear. It is certainly possible to continue the limit cycles of the averaged system in rectangular coordinates, but this defeats the purpose of time averaging.

4.4 Four-Mode Continuation Results

The results obtained by applying the continuation technique to the four-mode approximation to Equation (1.7) were significantly different than the results for the two-mode approximation. Figure 5 shows the limit cycle behavior of the four-mode approximation as a function of α_1. The results for the

corresponding two-mode approximation are shown in Figure 4. The most obvious difference between the two sets of results is that the stability boundary that occurred at the turning point bifurcation for the two-mode approximation does not exist for the four-mode approximation. For the four-mode approximation, a stable limit cycle exists for the entire range of values of α_1 studied.

In hindsight, it is not entirely surprising that the stability boundary determined by the two-mode approximation is sensitive to the number of acoustic modes included in the approximate system. The two-mode approximation, in which energy is produced by the linearly unstable first mode, η_1, then transported to the stable second mode, η_2, where it is subsequently dissipated is a gross approximation to the energy cascade that occurs in fluid dynamical systems. For slightly unstable systems (i.e. α_1 is small) the two-mode approximation is sufficient as can be seen by comparing Figure 4 and Figure 5. For more unstable systems (larger values of α_1) it becomes difficult for the second mode to dissipate the energy produced by the first mode. At some point it becomes impossible for the second mode to dissipate the energy produced by the first mode. As a result, the turning point bifurcation occurs beyond which no limit cycles exist.

In the four-mode approximation, the third and fourth acoustic modes are also able to dissipate energy, resulting in a system which contains stable limit cycles for larger values of α_1. When α_1 is near 131, the value at which the turning point occurs in the two-mode approximation, the amplitudes of the third and fourth acoustic modes are about ten percent of the mean chamber pressure. This is smaller than the amplitude of the second acoustic mode, but clearly significant to the energy balance in the limit cycle. Also note that the linear damping parameters of the higher-frequency modes are generally larger than the linear damping parameters of the lower-frequency modes (see Table I). Thus, as typical of fluid mechanical systems, higher frequency modes are more efficient at dissipating energy than lower frequency modes.

Figure 6 shows the time dependent amplitudes of the first two acoustic modes. The amplitudes seem to have sinusoidal time dependence as was seen in the two-mode approximation. It is interesting to note that the time dependent amplitude of the second acoustic mode has a DC offset from zero (see Figure 6b). This seems to be the case for all values of α_1 with the offset increasing for increasing values of α_1. The time dependent amplitude of the pressure fluctuation at the head of the combustor is also asymmetric about zero for values of α_1 larger than 200. It is important to note however that the maximum amplitude of the positive pressure fluctuation is larger than the mean pressure in the chamber, so the perturbation expansion used to derive the nonlinear acoustic equations is probably not valid. Also note that the maximum amplitude of the negative pressure fluctuation becomes larger than one when α_1 reaches 300, which is physically impossible. This underscores the importance of monitoring the amplitude of the pressure fluctuation to determine whether the results are physically realistic.

4.5 Six-Mode Continuation Results

In view of the major differences between the two- and four-mode approximations it seems prudent to determine the limit cycle behavior of the six-mode approximation to determine whether or not there are differences between the limit cycle behavior of the four- and six-mode approximations. Figure 7 shows the maximum time dependent amplitudes of the first two acoustic modes as functions of α_1 for the six-mode approximation. At first glance, the results for the six-mode approximation seem similiar to the results for the four-mode approximation. A limit cycle exists and is stable for the entire range of values of α_1 that were analyzed. On closer inspection however, one sees that the magnitude of the time dependent amplitudes is smaller for the six-mode approximation than for the four-mode approximation. This is particularly evident for values of α_1 larger than 200.

The rapid increase in the magnitude of the time dependent amplitudes that occurred near α_1 equal to 200 in the four-mode approximation is absent from the results for the six-mode approximation. In particular, the magnitude of the pressure fluctuation at the head of the chamber for α_1 equal to 300 is twice as large for the four-mode approximation as for the six-mode approximation. This occurs because when more modes are included in the truncated system more modes are available to dissipate energy. When an insufficient number of modes are included in the approximation each mode must dissipate the amount of energy it naturally would, plus some of the energy that would naturally be dissipated by higher-frequency modes. Thus the required number of modes to include in an approximation depends on the degree of instability of the system (i.e. the value of α_1). For larger values of α_1 it is necessary to include more modes in the approximation.

V. Results for a Second-Mode Instability

5.1 Two-Mode Approximation

The solution for the two-mode time-averaged equations is the same for a first- or second-mode instability, so the solution for the two-mode time-averaged system with an unstable second mode

is given by Equation (4.6). Stability boundaries for the two cases are different however. For the second-mode instability the solution is stable when (Paparizos and Culick[1])

$$\frac{(\beta^2-1)-\sqrt{(3\,\beta^2+1)(\beta^2-1)}}{(\beta^2+1)} < \frac{\alpha_2}{\alpha_1} < 0.$$

Generally the flow of energy in fluid mechanical systems is from low-frequency modes to high-frequency modes. In the present case the second mode is unstable so in the two-mode approximation energy is forced to flow from a higher-frequency mode to a lower-frequency mode. This is not physically realistic so it is unlikely that the two-mode approximation is a valid model of the fluid mechanics when the second mode is unstable. The insufficiencies of the two-mode approximation can be seen more clearly by looking at the asymptotic expansion of the two-mode approximation. Using Equation (1.7) it can be shown that the two-mode system is given by

$$\begin{aligned}
\dot{\eta}_1 &= \xi_1 \\
\dot{\xi}_1 &= 2\,\widehat{\alpha}_1\,\xi_1 - (1-2\widehat{\theta}_1)\eta_1 \\
&\quad - \left(\frac{3-2\,\gamma}{2\,\gamma}\right)\xi_1\,\xi_2 - \left(\frac{5\,(\gamma-1)}{2\,\gamma}\right)\eta_1\,\eta_2 \\
\dot{\eta}_2 &= \xi_2 \\
\dot{\xi}_2 &= 2\,\widehat{\alpha}_2\,\xi_2 - 4\,(1-\widehat{\theta}_2)\,\eta_2 \\
&\quad + \left(\frac{\gamma+3}{2\,\gamma}\right)\xi_1^2 - \left(\frac{\gamma-1}{2\,\gamma}\right)\eta_1^2.
\end{aligned} \tag{5.1}$$

Since small initial disturbances from the zero steady state will grow linearly it is useful to examine the solution of the linearized form of Equation (5.1). Linearizing Equation (5.1) about the origin results in the system

$$\begin{pmatrix} \dot{\eta}_1 \\ \dot{\xi}_1 \\ \dot{\eta}_2 \\ \dot{\xi}_2 \end{pmatrix} = \begin{pmatrix} 0 & 1 & 0 & 0 \\ -(1-2\,\widehat{\theta}_1) & 2\,\widehat{\alpha}_1 & 0 & 0 \\ 0 & 0 & 0 & 1 \\ 0 & 0 & -4\,(1-\widehat{\theta}_2) & 2\,\widehat{\alpha}_2 \end{pmatrix} \begin{pmatrix} \eta_1 \\ \xi_1 \\ \eta_2 \\ \xi_2 \end{pmatrix} \tag{5.2}$$

which has eigenvalues

$$\lambda_{1,2} = \widehat{\alpha}_1 \pm \mathbf{i}\sqrt{1-2\,\widehat{\theta}_1-\widehat{\alpha}_1^2} \;= \widehat{\alpha}_1 \pm \mathbf{i}\,\Omega_1$$

$$\lambda_{3,4} = \widehat{\alpha}_2 \pm \mathbf{i}\sqrt{1-\widehat{\theta}_2-(\widehat{\alpha}_2/2)^2} \;= \widehat{\alpha}_2 \pm \mathbf{i}\,\Omega_2.$$

Thus the solution to the linearized system has the form

$$\begin{aligned}
\begin{pmatrix} \eta_1 \\ \xi_1 \end{pmatrix} &= e^{\widehat{\alpha}_1 t}\left[\begin{pmatrix} a_1 \\ a_2 \end{pmatrix}\sin\Omega_1 t + \begin{pmatrix} b_1 \\ b_2 \end{pmatrix}\cos\Omega_1 t\right] \\
\begin{pmatrix} \eta_2 \\ \xi_2 \end{pmatrix} &= e^{\widehat{\alpha}_2 t}\left[\begin{pmatrix} a_3 \\ a_4 \end{pmatrix}\sin\Omega_2 t + \begin{pmatrix} b_3 \\ b_4 \end{pmatrix}\cos\Omega_2 t\right].
\end{aligned} \tag{5.3}$$

Solving for the constants a_i and b_i, $i = 1,\ldots,4$, for $\widehat{\alpha}_2$ equal to zero shows that the asymptotic solution of the two-mode approximation for $\widehat{\alpha}_2 << 1$ is

$$\begin{aligned}
\begin{pmatrix} \eta_1 \\ \xi_1 \end{pmatrix} &= \begin{pmatrix} 0 \\ 0 \end{pmatrix} \\
\begin{pmatrix} \eta_2 \\ \xi_2 \end{pmatrix} &= e^{\widehat{\alpha}_2 t}\begin{pmatrix} \frac{1}{\Omega_2}\sin\Omega_2 t + \cos\Omega_2 t \\ -\Omega_2\sin\Omega_2 t + \cos\Omega_2 t \end{pmatrix}
\end{aligned} \tag{5.4}$$

Only the second mode is linearly excited, as one would expect, because the acoustic modes are linearly uncoupled. Thus if the second mode is to excite the first mode it must do so through the nonlinear terms. An examination of the two-mode approximation [see Equation (5.1)] shows that the first mode is nonlinearly coupled to the second mode through the terms $\xi_1\xi_2$ and $\eta_1\eta_2$. With this form of coupling it is not possible for the second mode to excite the first mode if the first mode is initially unexcited. This is not the case for energy transfer from the first mode to the second mode. In that case the nonlinear coupling terms are η_1^2 and ξ_1^2, so if the first mode becomes excited energy will be transported to the second mode. This corresponds to the physical situation where energy is transported from low-frequency modes to high-frequency modes.

Based on the above discussion it seems reasonable to assume that modes of order greater than two must be included in the analysis of the second-mode instability. Enough modes must be included in the approximation to allow for the natural flow of energy between modes. By expanding Equation (1.7) for a four-mode approximation one can show that nonlinear terms of the form η_2^2 and ξ_2^2 transfer energy from the second mode to the fourth mode when only the second mode is excited. Thus the natural mode of energy transfer for the second-mode instability is from the unstable second mode to the stable fourth mode.

5.2 Four-Mode Time-Averaged Results

The four-mode time-averaged equations determined from Equation (1.9) are

$$\begin{aligned}
\dot{A}_1 &= \widehat{\alpha}_1\,A_1 + \widehat{\theta}_1\,B_1 \\
&\quad - \kappa\big[A_1\,A_2 + B_1\,B_2 + A_2\,A_3 + B_2\,B_3 \\
&\qquad + A_3\,A_4 + B_3\,B_4\big] \\
\dot{B}_1 &= \widehat{\alpha}_1\,B_1 - \widehat{\theta}_1\,A_1 \\
&\quad + \kappa\big[B_1\,A_2 - A_1\,B_2 + B_2\,A_3 - A_2\,B_3 \\
&\qquad + B_3\,A_4 - A_3\,B_4\big] \\
\dot{A}_2 &= \widehat{\alpha}_2\,A_2 + \widehat{\theta}_2\,B_2 \\
&\quad + 2\kappa\big[\tfrac{1}{2}\,(A_1^2 - B_1^2) - A_1\,A_3 - B_1\,B_3 \\
&\qquad - A_2\,A_4 - B_2\,B_4\big]
\end{aligned}$$

$$
\begin{aligned}
\dot{B}_2 &= \widehat{\alpha}_2 B_2 - \widehat{\theta}_2 A_2 \\
&\quad + 2\kappa\left[A_1 B_1 + A_3 B_1 - A_1 B_3 + A_4 B_2 - A_2 B_4\right] \\
\dot{A}_3 &= \widehat{\alpha}_3 A_3 + \widehat{\theta}_3 B_3 \\
&\quad + 3\kappa\left[A_1 A_2 - B_1 B_2 - A_1 A_4 - B_1 B_4\right] \\
\dot{B}_3 &= \widehat{\alpha}_3 B_3 - \widehat{\theta}_3 A_3 \\
&\quad + 3\kappa\left[A_1 B_2 + A_2 B_1 + A_4 B_1 - A_1 B_4\right] \\
\dot{A}_4 &= \widehat{\alpha}_4 A_4 + \widehat{\theta}_4 B_4 \\
&\quad + 4\kappa\left[A_1 A_3 - B_1 B_3 + \frac{1}{2}(A_2^2 - B_2^2)\right] \\
\dot{B}_4 &= \widehat{\alpha}_4 B_4 - \widehat{\theta}_4 A_4 \\
&\quad + 4\kappa\left[A_1 B_3 + A_2 B_2 + A_3 B_1\right]
\end{aligned}
\tag{5.5}
$$

where

$$\kappa = \frac{\gamma + 1}{8\,\gamma}.$$

For the case of a second-mode instability, an initial disturbance of the second acoustic mode will grow and result in an increase of energy in the system. The energy produced by the unstable second mode will be transported to the other acoustic modes throught the nonlinear coupling terms. An examination of Equation (5.5) shows that if the first, third, and fourth acoustic modes are initially unexcited while the second acoustic mode is excited, then energy will be transported from the second mode to the fourth mode but no energy will be transported from the second mode to either the first mode or the third mode. This can be seen by setting A_1, B_1, A_3, B_3, A_4, and B_4 equal to zero in Equation (5.5) to obtain

$$
\begin{aligned}
\dot{A}_1 &= 0 \\
\dot{B}_1 &= 0 \\
\dot{A}_2 &= \widehat{\alpha}_2 A_2 + \widehat{\theta}_2 B_2 \\
\dot{B}_2 &= \widehat{\alpha}_2 B_2 - \widehat{\theta}_2 A_2 \\
\dot{A}_3 &= 0 \\
\dot{B}_3 &= 0 \\
\dot{A}_4 &= 2\,\kappa\left[A_2^2 - B_2^2\right] \\
\dot{B}_4 &= 4\,\kappa\left[A_2 B_2\right].
\end{aligned}
\tag{5.6}
$$

Further examination of Equation (5.5) reveals that if the second and fourth modes are excited but the first and third modes are initially unexcited, then the first and third modes will remain unexcited for all time. From this simple analysis it appears that in the time averaged equations the even acoustic modes are unable to excite the odd acoustic modes.

Since the odd acoustic modes can remain unexcited when the even acoustic modes are excited one can look for steady states of Equation (5.5) for which A_1, B_1, A_3, and B_3 are identically zero. Equation (5.5) then reduces to the two-mode system

$$
\begin{aligned}
\dot{A}_2 &= \widehat{\alpha}_2 A_2 + \widehat{\theta}_2 B_2 - 2\,\kappa\left[A_2 A_4 + B_2 B_4\right] \\
\dot{B}_2 &= \widehat{\alpha}_2 B_2 - \widehat{\theta}_2 A_2 + 2\,\kappa\left[A_4 B_2 - A_2 B_4\right] \\
\dot{A}_4 &= \widehat{\alpha}_4 A_4 + \widehat{\theta}_4 B_4 + 2\,\kappa\left[A_2^2 - B_2^2\right] \\
\dot{B}_4 &= \widehat{\alpha}_4 B_4 - \widehat{\theta}_4 A_4 + 4\,\kappa\left[A_2 B_2\right]
\end{aligned}
\tag{5.7}
$$

which has the same form as the two-mode time-averaged system composed of the first and second acoustic modes. Thus the solution of the two-mode system composed of the first and second modes, Equation (4.6), can be used to obtain the solution to Equation (5.7). Replacing the subscripts 1 and 2 in Equation (4.6) with 2 and 4, respectively, and replacing κ by 2κ the solution to the four-mode time-averaged approximation can be shown to be

$$
\begin{aligned}
&\eta_1(t) = 0 \\
&\eta_2(t) = \\
&\qquad \frac{8\,\gamma}{(\gamma+1)\,\omega_2}\sqrt{-\alpha_2\,\alpha_4\,(1+\beta^2)}\,\sin\left(\omega_2 t + \phi_2(t)\right) \\
&\eta_3(t) = 0 \\
&\eta_4(t) = \\
&\qquad \frac{8\,\gamma}{(\gamma+1)\,\omega_2}\sqrt{\alpha_2^2\,(1+\beta^2)}\,\sin\left(2\,\omega_2 t + \phi_4(t)\right)
\end{aligned}
\tag{5.8}
$$

where

$$
\begin{aligned}
\phi_2(t) &= -\left(\frac{\alpha_2\,\theta_4 + \alpha_4\,\theta_2}{2\,\alpha_2 - \alpha_4}\right) t + \phi_{20} \\
\phi_4(t) &= -2\left(\frac{\alpha_2\,\theta_4 + \alpha_4\,\theta_2}{2\,\alpha_2 - \alpha_4}\right) t + \phi_{40} \\
\beta &= \left(\frac{\theta_4 - 2\,\theta_2}{\alpha_4 + 2\,\alpha_2}\right)
\end{aligned}
$$

and

$$2\,\phi_{20} - \phi_{40} = \tan^{-1}(-\beta).$$

The analysis of this solution is the same as that given in Section 4.1 for the case of an unstable first mode and a stable second mode.

5.3 Four-Mode Continuation Results

Results for the four-mode approximation are obtained by expanding Equation (1.7) for $n = 1, 2, 3, 4$ and then using the continuation method to determine the limit cycles of the resulting eighth-order system. A branch of limit cycles arises from the Hopf bifurcation point that occurs when α_2 is zero. Figure 8 shows the results of the continuation method along with the results from the time-averaged equations. Recall that the four-mode time-averaged equations were solved by setting the first and third modes equal to zero and solving the resulting two-mode system consisting of the second and fourth modes.

Figure 8 shows that the time dependent amplitudes of the first and third modes are zero

in the limit cycles predicted by the continuation method. This matches the solution of the time-averaged equations. The maximum amplitudes of the second and fourth modes in the limit cycle are essentially the same for the time averaged and non-time averaged systems when α_2 is less than 75. For values of α_2 larger than 75, the limit cycles predicted by the two methods start to diverge. The maximum amplitudes of η_2 and η_4 in the limit cycle predicted by the continuation method are larger than the maximum amplitudes of η_2 and η_4 predicted by time averaging. Stability boundaries predicted by the two methods are substantially different for the two systems. The stability boundary predicted by the continuation method occurs at α_2 equal to 109, while time averaging predicts a stability boundary at α_2 equal to 140. Thus while time averaging predicts a stability boundary when α_4/α_2 equals -2, the continuation method predicts a stability boundary when α_4/α_2 equals -2.6.

5.4 Six-Mode Continuation Results

Figure 9 shows the maximum amplitudes of the acoustic modes in the limit cycle as functions of α_2 for the six-mode approximation, corresponding to those given in Figure 8 for the four-mode approximation. For values of α_2 less than 84 the limit cycles for the four- and six-mode approximations are similiar. The odd modes remain unexcited for both systems, while the even modes increase in amplitude as α_2 increases. For values of α_2 greater than 84, the limit cycles of the four- and six-mode approximations are qualitatively different. A pitchfork bifurcation of the limit cycles of the six-mode approximation occurs at a value of α_2 of 84. This pitchfork bifurcation results in the formation of a stable branch of limit cycles on which the odd modes are excited. Thus for values of α_2 greater than 84, one would expect the amplitudes of the odd modes to be nonzero in the limit cycle. This is not the case for the four-mode approximation. In that case the odd modes remained zero for all values of α_2 studied. This should serve as a warning about making *a priori* assumptions about the solutions of nonlinear dynamical systems. If the odd modes had been assumed zero for all limit cycles in the six-mode continuation results, the pitchfork bifurcation would not have been found.

As a result of the pitchfork bifurcation, two separate branches of limit cycles exist for values of α_2 greater than 84. On what will be called the primary branch, the odd modes have zero amplitude in the limit cycle. This branch exists for all values of α_2 and appears as a result of the Hopf bifurcation that occurs when α_2 equals zero. The limit cycles on this branch are stable up to the pitchfork bifurcation that occurs at α_2 equal to 84, and unstable for values of α_2 larger than 84. For the branch of limit cycles that occur as a result of the pitchfork bifurcation, here called the secondary branch, the odd modes have nonzero amplitudes. Since the odd modes are linearly stable, and thus able to dissipate energy when they are excited, the amplitudes of the even modes are smaller on the secondary branch than on the primary branch.

The secondary branch is linearly stable for values of α_2 from 84 to 155. A torus bifurcation occurs on the secondary branch at a value of α_2 of 155 causing the limit cycles to be unstable when α_2 is greater than 155. As a result of the torus bifurcation, a branch of toroidal solutions will appear for values of α_2 greater than 155. Figure 10 shows a time simulation for α_2 equal to 160. Multiple frequencies are clearly evident in the time simulation. The high-frequency content corresponds to the acoustic frequency of the combustion chamber, while the low-frequency content is a result of the torus bifurcation. It is difficult to assign any physical meaning to the low-frequency oscillations as the toriodal motion is highly nonlinear. Figure 11 shows a Poincare map of the time simulation of Figure 10. The closed orbit in Figure 11 clearly shows that the motion is toriodal for α_2 equal to 160.

For values of α_2 larger than 160 the time dependent amplitudes of the acoustic modes seem to become chaotic. Figure 12 shows a time simulation for α_2 equal to 201.55. This value of α_2 is larger than the value at which the toroidal motion occurs, so the chaotic type behavior could be the result of a bifurcation of the toroidal motion. There is no simple way to determine whether the toroidal motion undergoes a bifurcation; this remains an open question. Note that any possible bifurcation of the toroidal motion occurs when α_2 is greater than 160, which corresponds to large values of η_n and ξ_n. Thus the six-mode approximation may not be sufficient to describe the nonlinear acoustic behavior in this region. Adding more modes to the approximation may change the qualitative behavior of the system, as was shown above, so the next task will be to analyze a system of more than six mode to determine whether or not the qualitiative nature of the limit cycles changes.

VI. Conclusions

One major result of this analysis has been to show that for a first-mode instability the stability boundaries predicted with the two-mode time-averaged equations are artifacts of the two-mode approximation. A stability boundary is also found when the continuation technique is used to calculate the limit cycles of the two mode non-time averaged equations, so the existence of the stability boundary is characteristic of the two-mode approximation and is not the result of time averaging. Time averaging does introduce some error as there is a

significant difference between the values of α_1/α_2 at which the stability boundary occurrs for the time-averaged and non-time averaged two-mode approximations. There is also a difference in the maximum amplitudes of the limit cycles for the two sets of equations.

No stability boundary is found for the four- or six-mode continuation results for the case of an unstable first mode. A limit cycle exists and is stable for all values of α_1 examined in this study. There is a significant difference in the magnitude of the time dependent amplitudes of the acoustic modes in the limit cycle for the four- and six-mode approxmations for large values of α_1. Figure 13 shows a comparison of the maximum positive amplitude of η_1 in the limit cycle as a function of α_1 for the two-, four-, and six-mode approximations. In the neighborhood of the Hopf bifurcation point (α_1=0) the results of the various approximations are almost identical. The results of the different approximations begin to diverge when α_1 becomes larger than 20, but they remain relatively close for values of α_1 less than 100. Results of the four- and six-mode approximations diverge rapidly as α_1 becomes larger than 160. Figure 13 clearly shows that for larger values of α_1 (i.e. more unstable systems) it is necessary to include more modes in the approximate system. More modes are necessary to dissipate the additional energy produced by the more unstable first mode.

In the case of the second-mode instability, it has been found that the two-mode approximation consisting of the first and second acoustic modes is not physically realistic. This system does not allow for the natural transfer of energy from low-frequency to high-frequency modes, and it is not possible for the second mode to excite the first mode if the first mode is initially unexcited. An examination of the equations representing the time evolution of the time dependent amplitudes of the acoustic modes shows that when the second acoustic mode is unstable, linear energy transfer will occur from the unstable second mode to the stable fourth mode. There is no mechanism with the present dynamical system for the second and fourth acoustic modes to excite the first and third acoustic modes if the first and third acoustic modes are initially unexcited. Thus the four-mode approximation reduces to a two-mode system consisting of the second and fourth modes.

Results for the six-mode approximation with a second-mode instability predict limit cycle behavior not seen before. A pitchfork bifurcation of the primary branch occurs for α_2 equal to 84 and results in a new branch of limit cycles that have odd modes with nonzero amplitudes in the limit cycle. Thus for α_2 greater than 84 it is possible for energy to flow from the even modes to the odd modes. This new branch of limit cycles contains a torus bifurcation resulting in quasi-periodic motions. Similiar to the case of the first-mode instability, the number of modes required in an analysis of the second-mode instability depends on the degree of instability of the system.

References

1. Paparizos, L. and Culick, F. , "The Two-Mode Approximation to Nonlinear Acoustics in Combustion Chambers I. Exact Solution for Second Order Acoustics," *Combustion Science and Technology*, Vol. 65, 1989, pp. 39-65.
2. Guckenheimer, J. and Holmes, P., *Nonlinear Oscillations, Dynamical Systems, and Bifurcations of Vector Fields.* Springer-Verlag, New York, 1983.
3. Ioos, G. and Joseph, D., *Elementary Stability and Bifurcation Theory.* Springer-Verlag, New York, 1980.
4. Doedel, E. and Kernevez, J., "Software for Continuation Problems in Ordinary Differential Equations with Applications," Preprint, CALTECH, 1984.
5. Press, W. H., Flannery, B. P., Teukolsky, S. A., and Vetterling, W. T.,*Numerical Recipes — The Art of Scientific Computing*, Cambridge University Press, 1989.
6. Jahnke, C. C., "Analysis of the Second Order Nonlinear Acoustic Equations With Two Modes," CALTECH, Guggenheim Jet Propulsion Center Documents on Active Control of Combustion Instabilities, Document No. CI90-1, 1990.

TABLE I

First-Mode Instability

$\alpha_1 = 0 \rightarrow 300\ s^{-1}$	$\alpha_2 = -324.8\ s^{-1}$	$\alpha_3 = -583.6\ s^{-1}$
$\alpha_4 = -889.4\ s^{-1}$	$\alpha_5 = -1262.7\ s^{-1}$	$\alpha_6 = -1500\ s^{-1}$
$\theta_1 = 12.9\ rad/s$	$\theta_2 = 46.8\ rad/s$	$\theta_3 = -29.3\ rad/s$
$\theta_4 = -131.0\ rad/s$	$\theta_5 = -280.0\ rad/s$	$\theta_6 = -300.0\ rad/s$
$\omega_1 = 5654.87\ rad/s$		

Second-Mode Instability

$\alpha_1 = -84.9\ s^{-1}$	$\alpha_2 = 0 \rightarrow 300\ s^{-1}$	$\alpha_3 = -161.0\ s^{-1}$
$\alpha_4 = -279.4\ s^{-1}$	$\alpha_5 = -329.7\ s^{-1}$	$\alpha_6 = -520.2\ s^{-1}$
$\theta_1 = -66.7\ rad/s$	$\theta_2 = 12.9\ rad/s$	$\theta_3 = 108.2\ rad/s$
$\theta_4 = 46.8\ rad/s$	$\theta_5 = 8.8\ rad/s$	$\theta_6 = -29.3\ rad/s$
$\omega_1 = 2827.435\ rad/s$		

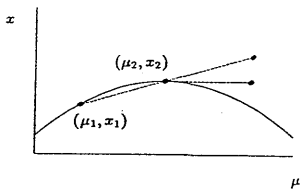

Figure 1: Graphical representation of continuation method.

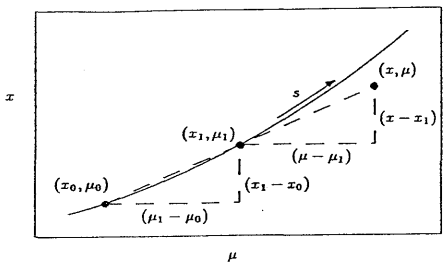

Figure 2: Graphical representation of approximation to the pseudo arc-length continuation equation.

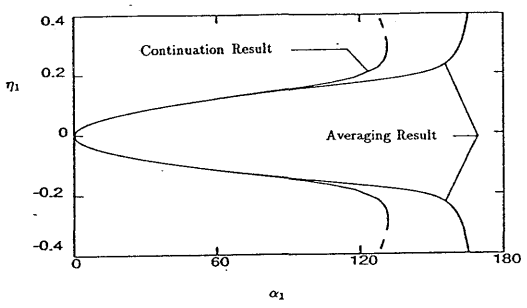

(a) Maximum amplitude of η_1

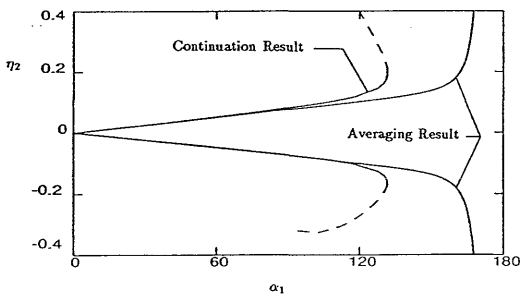

(b) Maximum amplitude of η_2

Figure 4: Maximum amplitudes of acoustic modes in limit cycle for two mode approximation,
—— Stable, - - - Unstable.

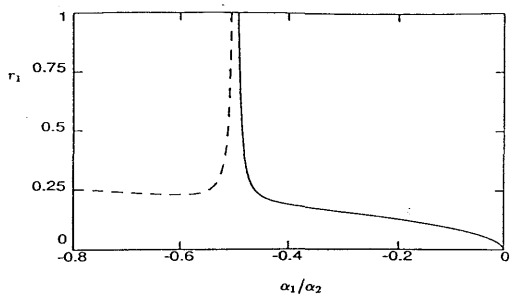

(a) Maximum amplitude of η_1

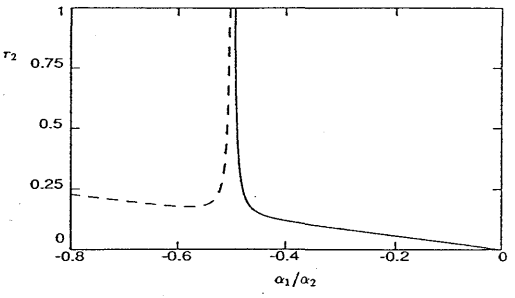

(b) Maximum amplitude of η_2

Figure 3: Maximum amplitudes of acoustic modes in limit cycle for two mode time averaged approximation,
—— Stable, - - - Unstable.

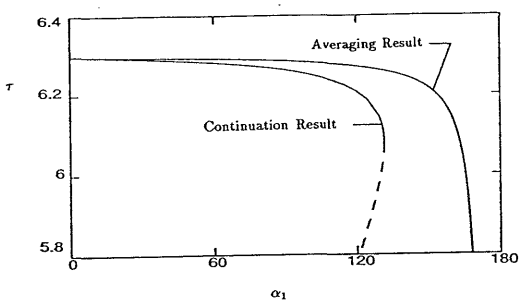

(c) Period of limit cycle

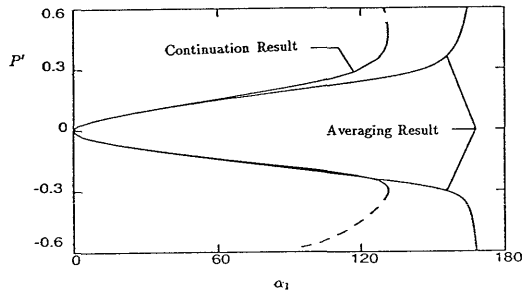

(d) Maximum amplitude of $P'(x = 0, t)$

Figure 4: Concluded.

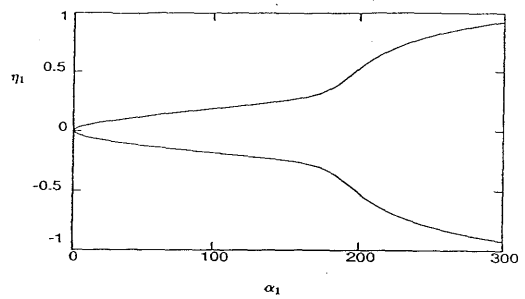

(a) Maximum amplitude of η_1

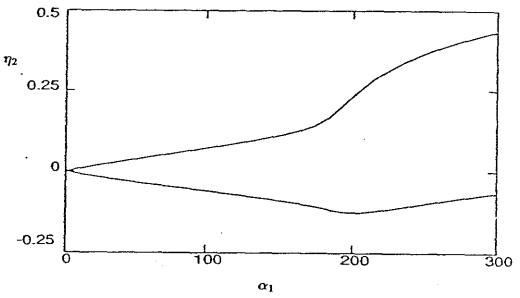

(b) Maximum amplitude of η_2

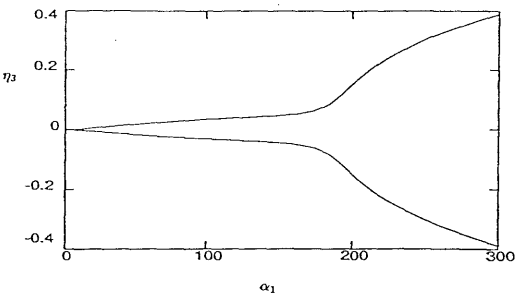

(c) Maximum amplitude of η_3

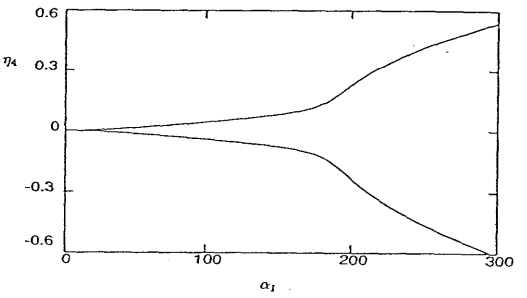

(d) Maximum amplitude of η_4

Figure 5: Maximum amplitudes of acoustic modes in limit cycle for four mode approximation, —— Stable, - - - Unstable.

Figure 5: Continued.

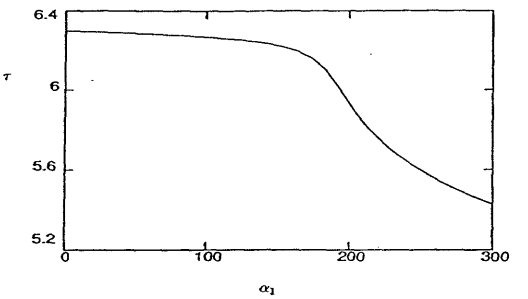

(e) Period of limit Cycle

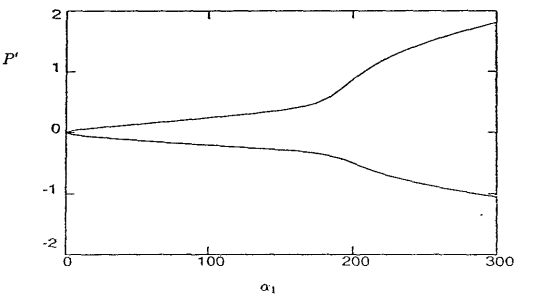

(f) Maximum amplitude of $P'(x=0,t)$

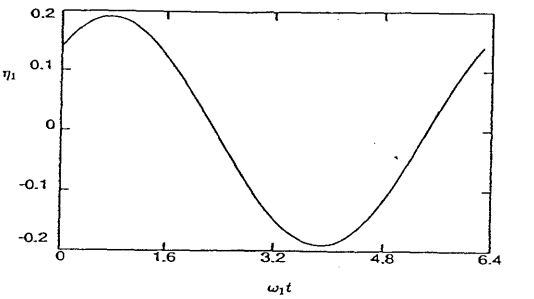

(a) Amplitude of η_1

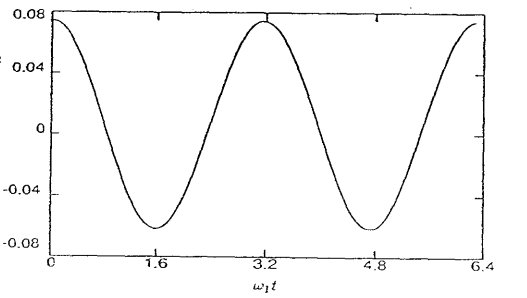

(b) Amplitude of η_2

Figure 5: Concluded.

Figure 6: Time dependent amplitudes of acoustic modes in limit cycle obtained with continuation method for four mode approximation, α_1=103.7.

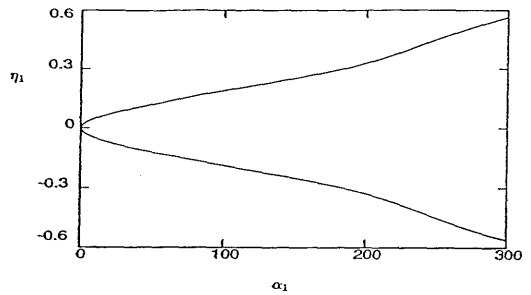

(a) Maximum amplitude of η_1

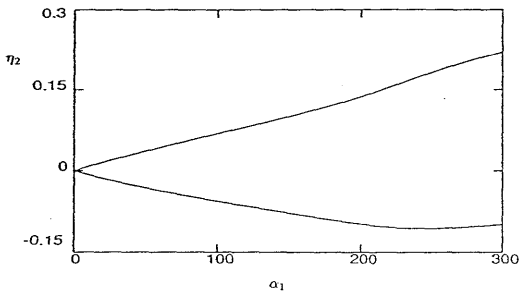

(b) Maximum amplitude of η_2

Figure 7: Maximum amplitudes of acoustic modes in limit cycle for six mode approximation, —— Stable, – – – Unstable.

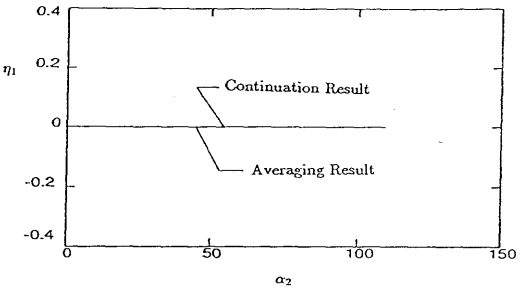

(a) Maximum amplitude of η_1

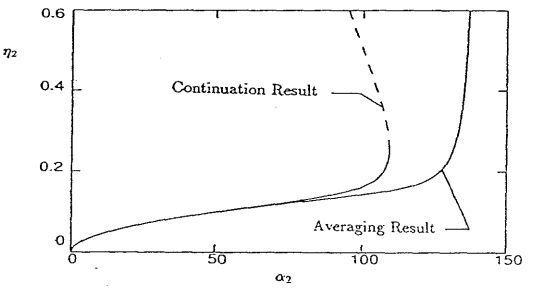

(b) Maximum amplitude of η_2

Figure 8: Maximum amplitudes of acoustic modes in the limit cycle for four mode approximation, —— Stable, – – – Unstable.

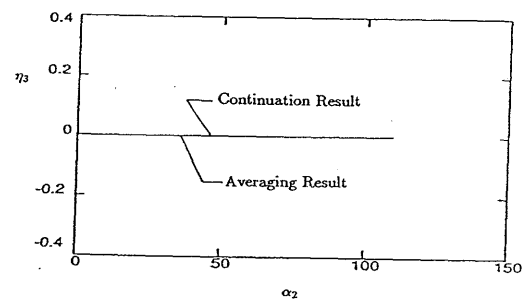

(c) Maximum amplitude of η_3

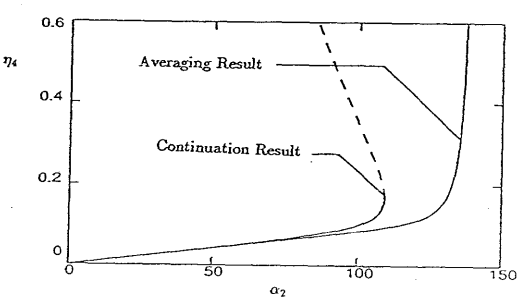

(d) Maximum amplitude of η_4

Figure 8: Continued.

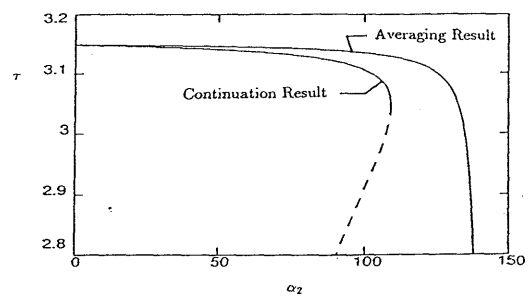

(e) Period of limit cycle

Figure 8: Concluded.

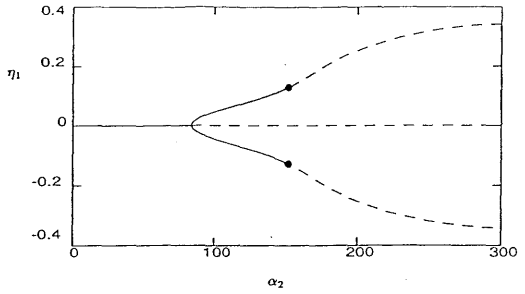

(a) Maximum amplitude of η_1

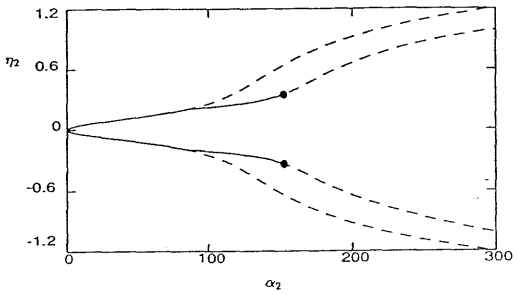

(b) Maximum amplitude of η_2

Figure 9: Maximum amplitudes of acoustic modes in limit cylce for six mode approximation, —— Stable, – – – Unstable, • - Torus Bifurcation.

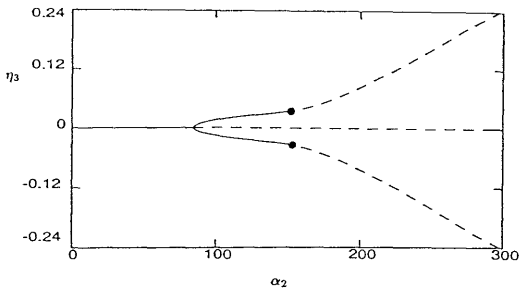

(c) Maximum amplitude of η_3

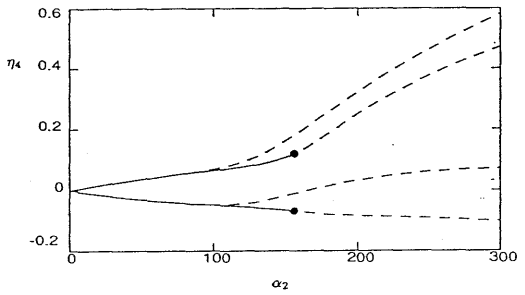

(d) Maximum amplitude of η_4

Figure 9: Continued.

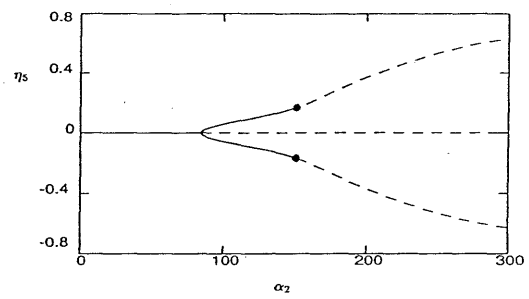

(e) Maximum amplitude of η_5

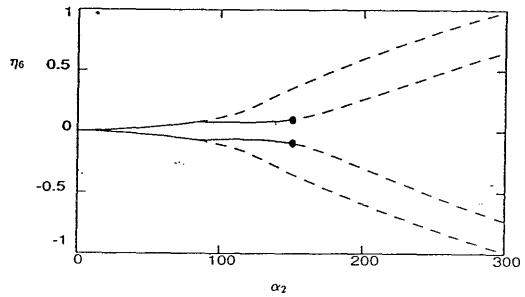

(f) Maximum amplitude of η_6

Figure 9: Continued.

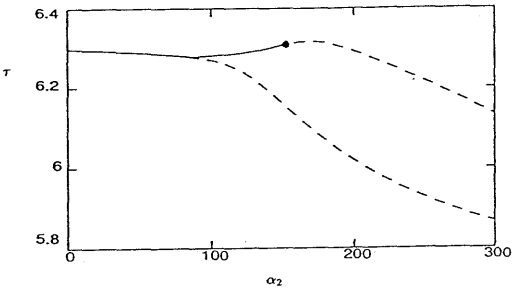

(g) Period of limit cycle

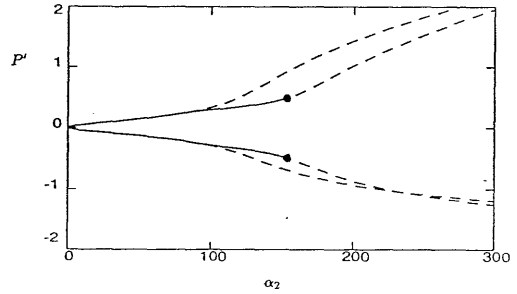

(h) Maximum amplitude of $P'(x=0,t)$

Figure 9: Concluded.

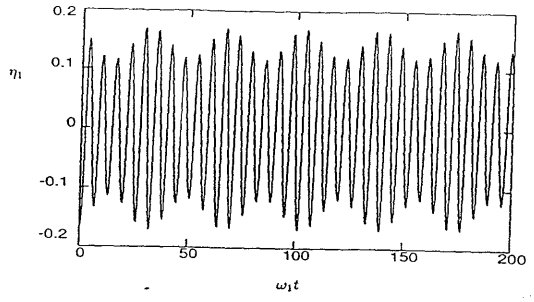

(a) Amplitude of η_1

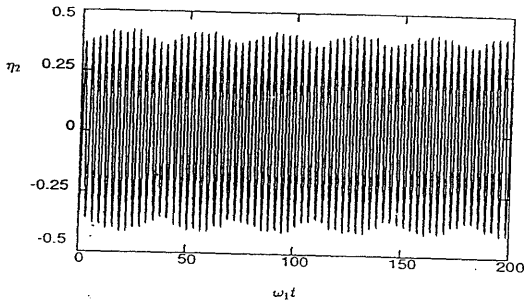

(b) Amplitude of η_2

Figure 10: Time simulation for the six mode approximation with $\alpha_2 = 160$.

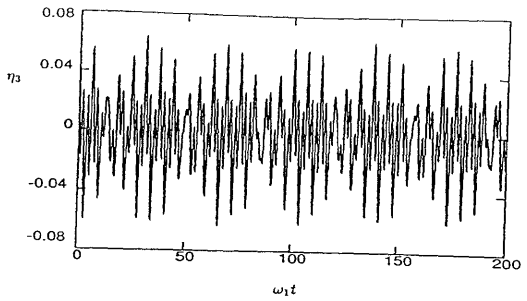

(c) Amplitude of η_3

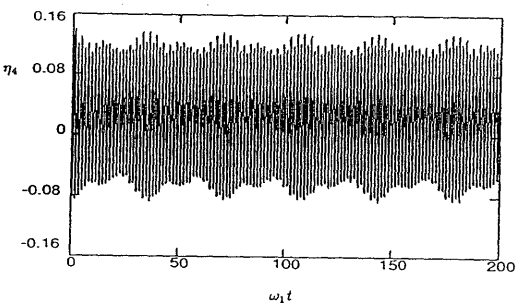

(d) Amplitude of η_4

Figure 10: Continued.

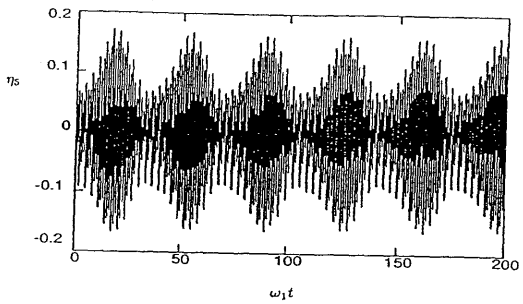

(e) Amplitude of η_5

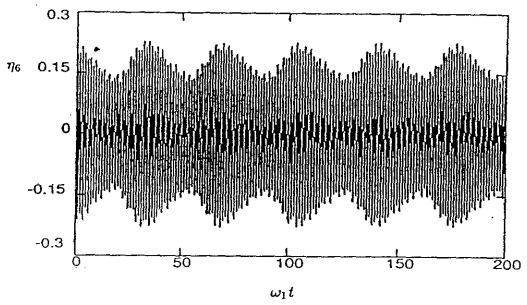

(f) Amplitude of η_6

Figure 10: Concluded.

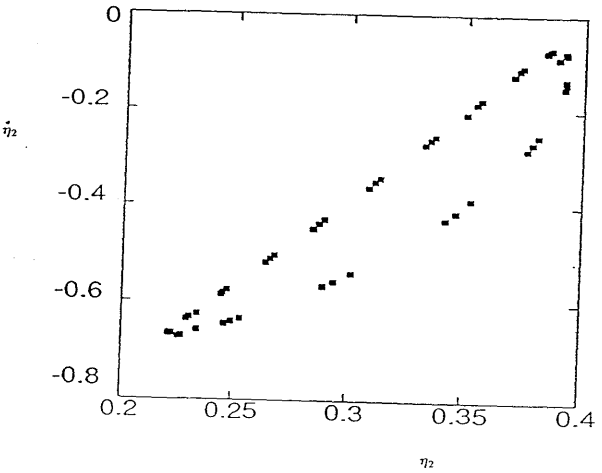

Figure 11: Poincare map of the time simulation of the six mode approximation with $\alpha_2 = 160$.

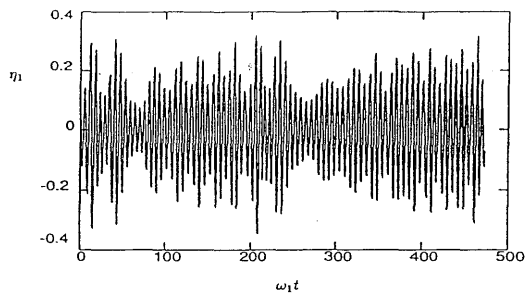

(a) Amplitude of η_1

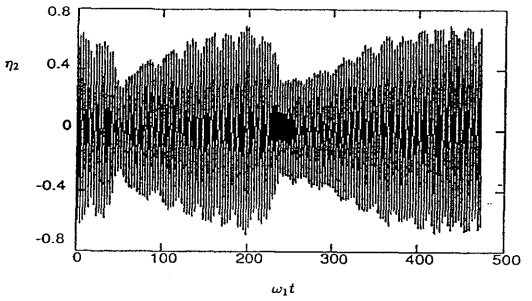

(b) Amplitude of η_2

Figure 12: Time simulation for the six mode approximation with $\alpha_2 = 201.55$.

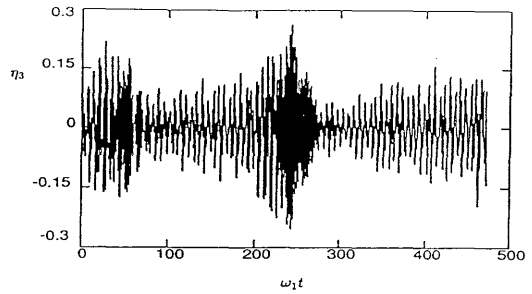

(c) Amplitude of η_3

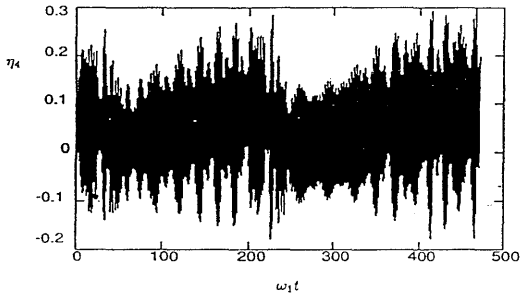

(d) Amplitude of η_4

Figure 12: Continued.

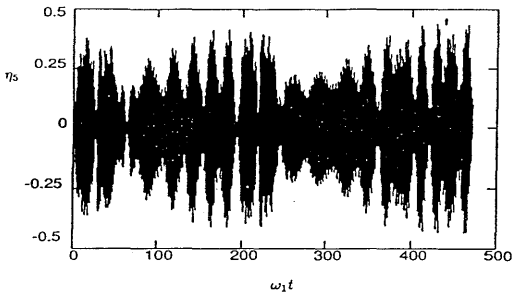

(e) Amplitude of η_5

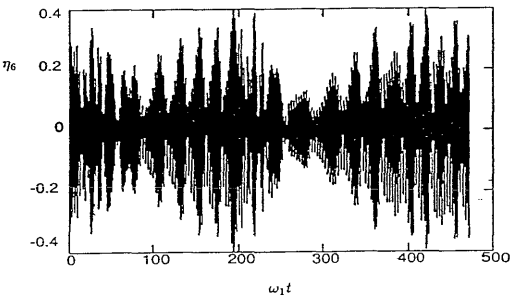

(f) Amplitude of η_6

Figure 12: Concluded.

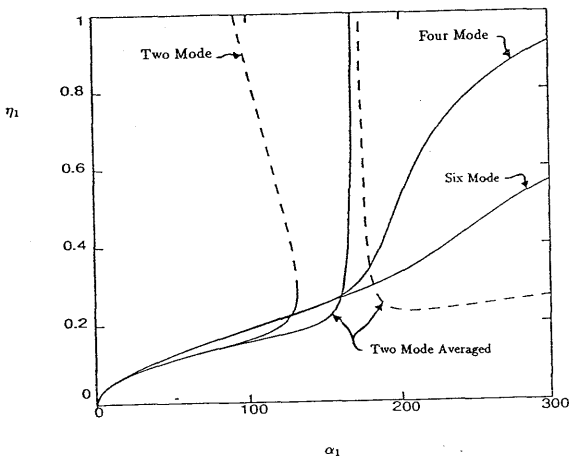

Figure 13: Comparison of maximum time dependent amplitudes of first acoustic mode for a first mode instability.